Available online at www.sciencedirect.com
ScienceDirect
Ceramics International 37 (2011) 1501–1505
CERAMICS INTERNATIONAL
www.elsevier.com/locate/ceramint

Incorporation of the transition metals (Cr and Fe) into β-SiAlON crystal structure

Hilmi Yurdakul, Servet Turan *

Anadolu University, Department of Materials Science and Engineering, Iki Eylul Campus, 26480 Eskisehir, Turkey

Received 3 November 2010; received in revised form 11 November 2010; accepted 4 January 2011
Available online 3 February 2011

Abstract

Outstanding properties for SiAlON ceramics can be obtained by tailoring the microstructure through α-SiAlON and β-SiAlON phase content as well as a type of secondary phases. It is so far well known that while some of the elements could be accommodated in α-SiAlON structure, β-SiAlON does not easily accommodate different elements in its structure. In this work, SiAlON ceramics were produced by using β-Si_3N_4 starting powder containing small amount of iron and chromium and the possible incorporation of iron and chromium into β-SiAlON structure was investigated by using analytical transmission electron microscopy (TEM) techniques. As a result of analytical TEM analysis, it is found that transition metals (Cr and Fe) can enter into the β-SiAlON crystal structure.

Keywords: B. Electron microscopy; B. Spectroscopy; D. SiAlON; Transition metals (Cr and Fe)

1. Introduction

SiAlON ceramics have recently attracted increasing interest as promising engineering materials thanks to their outstanding mechanical properties, superior thermal stability, high creep resistance and good oxidation/corrosion performance [1,2]. It is well known that all these desired properties of SiAlONs are tailored by manipulating the microstructure, basically consisting of two distinct polymorphs (α-SiAlON and β-SiAlON) and secondary phases [1,2]. Despite the fact that many of the alkali, alkaline earth and rare earth elements are commonly found to be incorporated into the α-SiAlON [3,4], none of these elements exist in β-SiAlON [1,5]. On the contrary, this view has been changing with recent studies revealing that some of the rare earth elements such as Eu^{2+} and Ce^{3+} can be accommodated into the β-SiAlON [6–8]. Furthermore, alkali and alkaline earth ions, e.g., Li^{+}, Mg^{2+} and Ca^{2+} have been shown to be incorporated into the host lattice of β-SiAlON [9].

The transition metal oxides (Cr_2O_3 and Fe_2O_3) were used as sintering aids with the aim of stabilization of α-SiAlON phase in the production of sintered-bulk SiAlON ceramics [10,11]. However, it was observed that Cr_2O_3 and Fe_2O_3 did not stabilize the α-SiAlON phase [10,11]. Additionally, formation of Cr- and Fe-silicide phases were reported, but no information was mentioned about the incorporation possibilities of Cr and Fe into the β-SiAlON structure [10,11]. On the other hand, in a couple of studies intended for preparation of β-SiAlON powders from Fe_2O_3-bearing fly ashes and coal-mine schists [12,13], Fe were observed in the elemental analysis of β-SiAlON fibres and spherical particles using scanning electron microscope (SEM) attached with energy dispersive X-ray (EDX) spectrometer. However, SEM-EDX analysis in thick samples is unreliable due to the large beam broadening [14] and as a result of this; there is no direct claim for Fe incorporation into the β-SiAlON structure in these studies [12,13]. Also, a Mossbauer spectroscopy study related to β-SiAlON produced from iron containing clay expressed that iron was not present in β-SiAlON structure [15]. Moreover, no published data related to possible existence of Cr in the β-SiAlON structure is available.

Therefore, the aim of this paper is to investigate the possibility of the incorporation of transition metals (Cr and Fe) into the β-SiAlON structure by using more reliable TEM techniques in a SiAlON ceramic produced with the use of Fe and Cr containing β-Si_3N_4 starting powders.

* Corresponding author. Tel.: +90 222 321 3550x6356; fax: +90 222 323 9501.
E-mail address: sturan@anadolu.edu.tr (S. Turan).

0272-8842/$36.00
doi:10.1016/j.ceramint.2011.01.009

2. Experimental

The SiAlON ceramics were produced by sintering the starting Si_3N_4 and AlN powders mixed with multi-cation sintering additives, i.e., yittrium oxide (Y_2O_3), samarium oxide (Sm_2O_3) and calcium oxide (CaO) at 1940 °C for 1 h under 22 bar nitrogen atmosphere in a gas pressure sintering furnace. The more detailed information about composition and production method of SiAlON ceramics can also be found in previous studies [16,17]. However, in this study instead of high purity α-Si_3N_4, less pure β-Si_3N_4 containing transition metal (Fe and Cr) impurities was chosen as a starting powder to produce cost effective SiAlON ceramics. The total amounts of iron and chromium together in β-Si_3N_4 powder were around 1 wt%.

The densities of sintered pellets were measured by using Archimedes' principle. The phase identification in sintered samples was performed by using powder X-ray diffraction (XRD) technique (Rigaku RINT-2000). For analytical TEM investigations, the electron transparent specimen was prepared by mechanical polishing, followed by Ar-ion beam thinning and finally carbon coating (Leica Microsystems EM RES101). Afterwards, the sample was characterized by using 200 kV field emission TEM (JEOL JEM-2100F) equipped with STEM high angle annular dark field (STEM-HAADF) detector (Model 3000, Fischione), parallel electron energy loss spectrometer (PEELS) and energy filter (Gatan GIF Tridiem), and energy dispersive X-ray (EDX) spectrometer (JEOL JED-2300T). The hard X-ray aperture was inserted to reduce the X-rays emitted from the parts of microscope column and specimen holder. A corrector was also used to avoid drift during the EDX analysis.

3. Results and discussion

Density measurements showed that sintered pellets were almost fully dense (99.5%). From the XRD analysis, it was found that the starting β-Si_3N_4 powder was converted to SiAlON phases. The α/β SiAlON ratio was calculated [18] to be 8/92. Also, a very small amount of Fe–Cr bearing metal silicides was detected.

The microstructure of SiAlON sample, high resolution TEM image of one of the β-SiAlON grain, as well as experimental and matching theoretical selected area electron diffraction patterns (SAEDP) obtained from 0 0 0 1 direction of a β-SiAlON grain are given in Fig. 1. Considering the atomic number (*Z*)-contrast STEM-HAADF image in Fig. 1(a), the rare earth element rich silicon–aluminum–oxynitride phases were clearly observed as white regions when compared to β-SiAlON grains. The reason of this contrast in HAADF image is due to the fact that high atomic number sintering additive elements such as Y, Sm and Ca existing at grain boundaries and in the quadruple junctions scatter electrons much more than the β-SiAlON grains containing lighter elements.

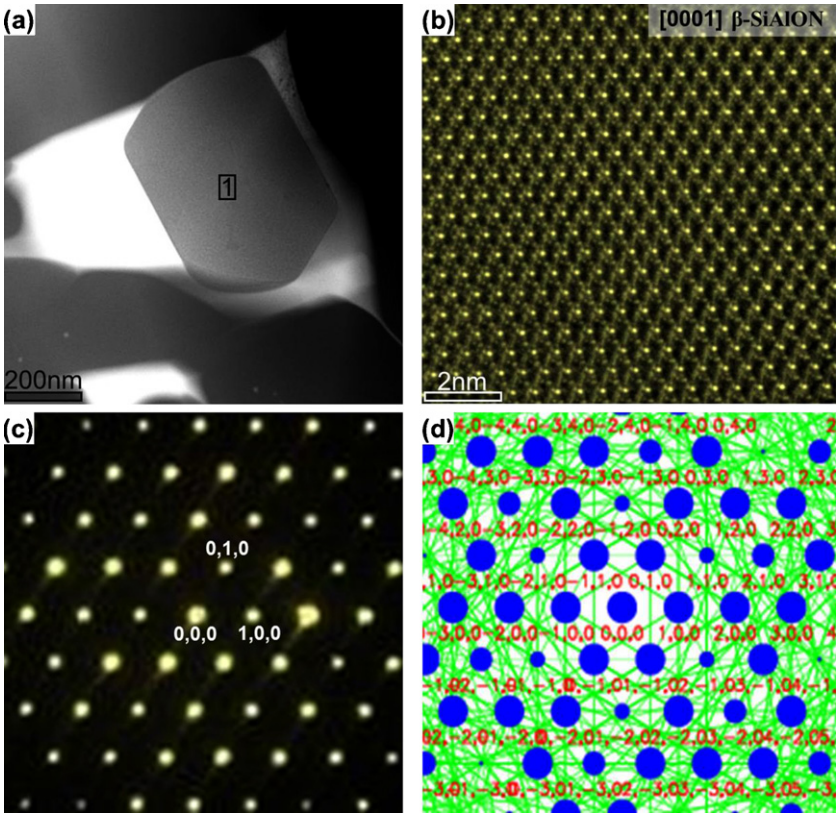

Fig. 1. (a) STEM-HAADF image showing the microstructure of SiAlON sample, (b) HREM image of β-SiAlON grain obtained from the rectangular region labelled with "1" in (a), (c) selected area electron diffraction pattern (SAEDP) of β-SiAlON acquired from the same grain and (d) kinematical SAEDP simulation of β-SiAlON along the [0 0 0 1] low index zone axis. Please note that Ref. [24] was used for the kinematical SAEDP simulation.

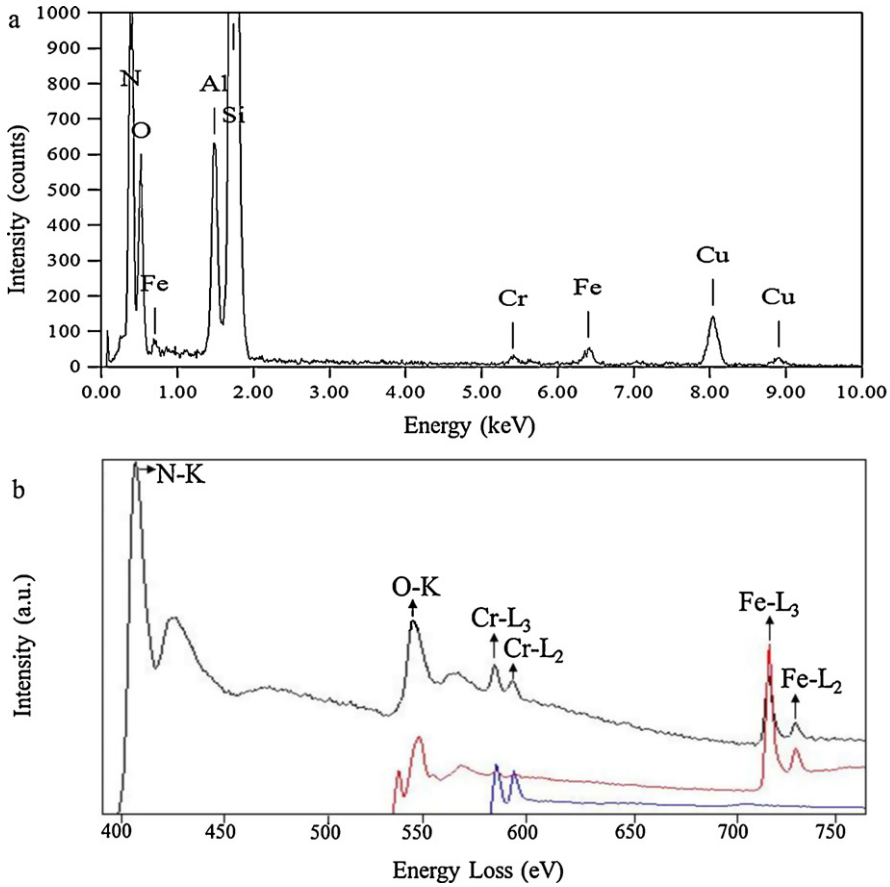

Fig. 2. (a) EDX spectrum and (b) EEL spectrum collected from the β-SiAlON grain marked with "1" in Fig. 1(a). EEL spectra of Fe_2O_3 (middle one) and Cr (bottom one) are also given in (b) as references. Please note that the diameter of electron beam used in STEM-based EDX and EELS spot analyses was about 1–2 nm and the backgrounds of EEL spectra were subtracted according to power-law [25].

Based on the EDX spectrum acquired from rectangular region marked with "1" in Fig. 1(a) and shown in Fig. 2(a), the grain was identified as β-SiAlON since the characteristic X-ray lines from α-SiAlON stabilizer elements such as Y, Sm and Ca were not visible in the spectrum. On the other hand, two explicit X-ray lines at approximately 5.4 keV and 6.4 keV corresponding to Cr Kα and Fe Kα, respectively, were detected along with expected peaks from β-SiAlON elements in the spectrum. More STEM-EDX analysis was also carried out from other β-SiAlON grains and their compositions are presented in Table 1. It can be seen that all the analysed grains contain Fe and Cr elements and furthermore from Table 1, the average composition of Fe and Cr containing β-SiAlON grains was calculated as $Fe_{0.58}Cr_{0.18}Si_{49.08}Al_{2.97}O_{6.67}N_{40.52}$ (at.%) by using standardless Cliff–Lorimer quantification method [19].

Nevertheless, to confirm the novelty of our results, EELS analysis was also carried out at the same region of β-SiAlON grain and compared with the reference EEL spectra of Fe_2O_3

Table 1
The quantitative STEM-EDX analysis of β-SiAlON grains.

β-SiAlON	Elements (at.%)						Composition
	Fe	Cr	Si	Al	O	N	
Grain-1	0.83	0.16	50.28	3.52	6.75	38.47	$Fe_{0.83}Cr_{0.16}Si_{50.28}Al_{3.52}O_{6.75}N_{38.47}$
Grain-2	0.82	0.18	54.06	3.27	3.91	37.76	$Fe_{0.82}Cr_{0.18}Si_{54.06}Al_{3.27}O_{3.91}N_{37.76}$
Grain-3	0.81	0.14	54.53	3.79	4.71	35.98	$Fe_{0.81}Cr_{0.14}Si_{54.53}Al_{3.79}O_{4.71}N_{35.98}$
Grain-4	0.80	0.19	49.22	2.82	5.27	41.25	$Fe_{0.80}Cr_{0.19}Si_{49.22}Al_{2.82}O_{5.27}N_{41.25}$
Grain-5	0.58	0.24	43.36	2.95	11.68	41.20	$Fe_{0.58}Cr_{0.24}Si_{43.36}Al_{2.95}O_{11.68}N_{41.20}$
Grain-6	0.55	0.17	56.60	0.65	6.53	35.61	$Fe_{0.55}Cr_{0.17}Si_{56.60}Al_{0.65}O_{6.53}N_{35.61}$
Grain-7	0.52	0.17	45.82	3.08	6.35	44.06	$Fe_{0.52}Cr_{0.17}Si_{45.82}Al_{3.08}O_{6.35}N_{44.06}$
Grain-8	0.33	0.14	41.49	3.55	9.09	45.40	$Fe_{0.33}Cr_{0.14}Si_{41.49}Al_{3.55}O_{9.09}N_{45.40}$
Grain-9	0.28	0.17	44.25	3.02	6.68	45.41	$Fe_{0.28}Cr_{0.17}Si_{44.25}Al_{3.02}O_{6.68}N_{45.41}$
Grain-10	0.18	0.11	51.33	3.09	5.29	40.01	$Fe_{0.18}Cr_{0.11}Si_{51.33}Al_{3.09}O_{5.29}N_{40.01}$
Average	0.58 ± 0.24	0.18 ± 0.03	49.08 ± 5.17	2.97 ± 0.87	6.67 ± 2.24	40.52 ± 3.62	$Fe_{0.58}Cr_{0.18}Si_{49.08}Al_{2.97}O_{6.67}N_{40.52}$

and Cr, taken from database of Gatan Digital Micrograph™ software (Fig. 2(b)). In view of the EEL spectrum at the top of Fig. 2(b), the Cr-$L_{3,2}$ and Fe-$L_{3,2}$ edges were clearly seen together with the N-K and O-K edges, which revealed that Cr and Fe existed in β-SiAlON grain. In addition, when Cr-$L_{3,2}$ and Fe-$L_{3,2}$ edges in β-SiAlON were compared in detail with reference EEL spectra in Fig. 2(b), it was determined that their features such as edge shape and positions were almost similar to the reference EEL spectra of Fe_2O_3 and Cr. Therefore, these findings present further evidence of Cr and Fe incorporation into the β-SiAlON structure. At this point, we state that Cr and Fe can be incorporated into the β-SiAlON structure. But, although Cr and Fe were found to be present by using the EDX and EELS analyses (Fig. 2), a question to be answered here is whether or not Cr and Fe signals were collected as an artefact from the parts of microscope column and/or specimen holder even though hard X-ray aperture were used.

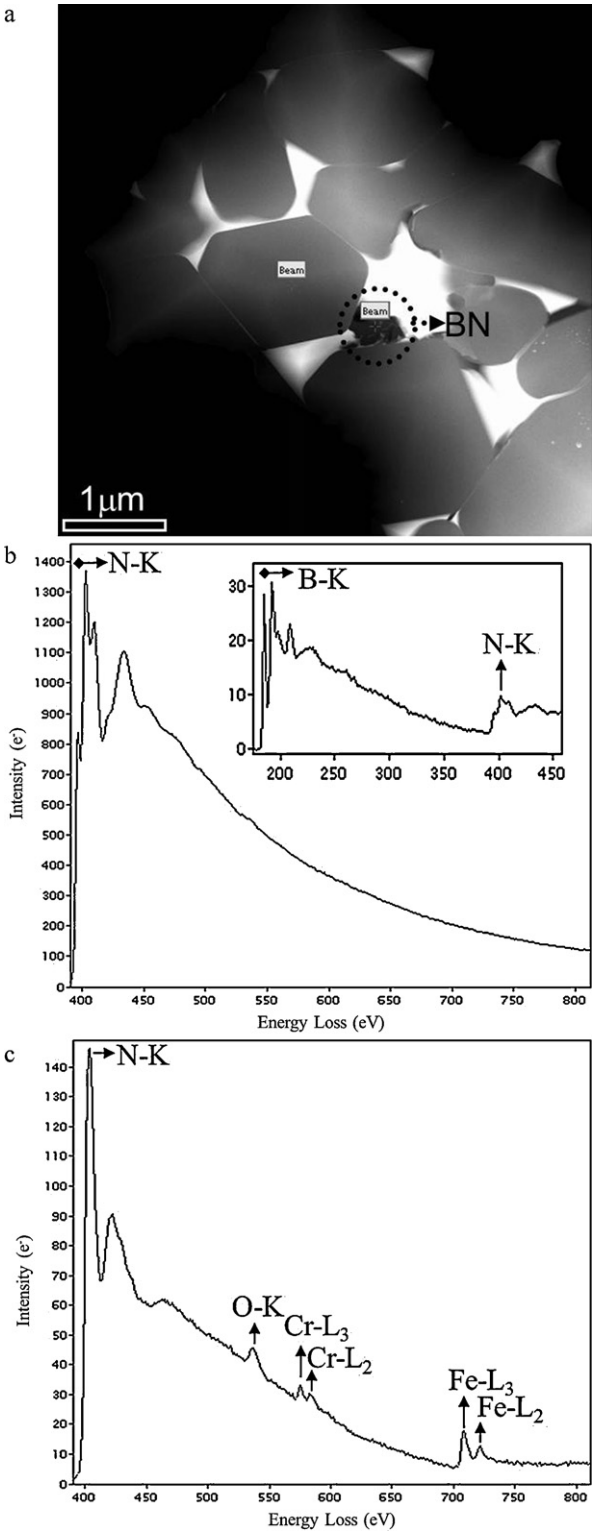

Fig. 3. (a) STEM-HAADF image showing the BN inclusion, (b) EEL spectrum acquired from the BN inclusion (inset image) in addition to detailed view of 400–800 eV energy loss range of N-K edge in inset image, and (c) EEL spectrum of β-SiAlON grain adjacent to BN inclusion. Please note that the beam positions for the EELS analysis for BN inclusion and β-SiAlON grain are also shown in (a).

In an attempt to clarify this point, we fortunately identified a boron nitride (h-BN) inclusion existing in the sample as a contaminant [20] from the BN spray used to cover the surface before sintering. Therefore, EELS analysis from the BN inclusion can be used as an internal standard to solve the problem whether Cr and Fe were identified as an artefact in the β-SiAlON grain. Thus, EELS analysis was carried out on the BN inclusions circled on the STEM-HAADF image in Fig. 3(a) and shown in Fig. 3(b) and compared with EEL spectrum from adjacent β-SiAlON grain (Fig. 3(c)). Looking at Fig. 3(c) showing the 570–740 eV energy loss ranges, the Cr-$L_{3,2}$ and Fe-$L_{3,2}$ edges were seen in the EEL spectrum of β-SiAlON grain whereas they were not visible in the EEL spectrum of BN inclusion (Fig. 3(b)) proving that Cr and Fe certainly entered into the β-SiAlON structure and they were not observed in β-SiAlON grains due to the artefacts.

Taking into consideration of experimental results presented herein, we think that variable ionic radii of Cr and Fe transition elements are key factor to understand how Cr and Fe can enter into the β-SiAlON structure. In to explain this phenomenon, it is sufficient to look at the ionic radii in fourfold coordination of Si^{4+} (26 pm) [21] and Al^{3+} (39 pm) [21] since they exist in the (Si, Al)(O, N)$_4$ tetrahedrons in the β-SiAlON crystal structure [22] and to compare with various ionic radii of Cr and Fe in fourfold coordination, e.g., Cr^{4+} (41 pm), Cr^{6+} (26 pm), Fe^{3+} (49 pm), and Fe^{6+} (25 pm) [21]. As a result of ionic radii comparison, it can be deduced that the incorporation of Cr and Fe into β-SiAlON crystal structure is possible with substitution mechanism in the (Si, Al)(O, N)$_4$ tetrahedrons. As a matter of fact, this view was discussed in a theoretical study [23] and explained that the incorporation of 3d-metal impurities can come true with a cation substitutional mechanism in silicon oxynitride (Si_2N_2O) structure [23].

Furthermore, it was shown that Eu^{2+} with an ionic radius of 117–135 pm depending on the coordination number [21] can enter as a single interstitial atom in the channels of β-SiAlON crystal structure [8]. Similarly, it might be possible that Cr and Fe atoms exist in the interstitial sites of β-SiAlON crystal structure because the ionic radii of Cr^{2+} (80 pm in sixfold coordination) [21] and Fe^{2+} (78 pm) [21] are smaller than the Eu^{2+} (117 pm in sixfold coordination). But, to determine the valance states of Cr and Fe and to decide where they exist in the β-SiAlON crystal structure, the detailed EELS analysis, atomic-resolved STEM-HAADF

imaging and further density functional theory (DFT) studies should be carried out.

Please also note that unfortunately we could not find α-SiAlON grains to investigate whether or not Fe and Cr also entered into the α-SiAlON grains.

4. Conclusions

The EDX and EELS analyses carried out in a TEM clearly showed that Fe and Cr can enter into the β-SiAlON structure. We believe that our results can be considered as a starting point for the initiation of new-generation SiAlON ceramics possessing different properties for different applications by means of transition metals incorporation into the β-SiAlON structure similar to rare-earth incorporated β-SiAlON materials [6,7] for white light-emitting diodes (LEDs).

Acknowledgement

The authors wish to express their gratitude to MDA ceramics (Turkey) for the provision of the samples.

References

[1] K.M. Fox, J.R. Hellmann, Microstructure and creep behavior of silicon nitride and SiAlONs, Int. J. Appl. Ceram. Technol. 5 (2008) 138–154.
[2] H. Mandal, F. Kara, S. Turan, A. Kara, Performance of new α–β SiAlONs in turning operations, Key Eng. Mater. 206–213 (2002) 929–932.
[3] S. Hampshire, H.K. Park, D.P. Thompson, K.H. Jack, α′-SiAlON ceramics, Nature 274 (1978) 880–882.
[4] S. Turan, H. Mandal, F. Kara, Transmission electron microscopy of SrO containing multi-cation doped alpha-SiAlON ceramics, Mater. Sci. Forum 383 (2002) 37–40.
[5] K.H. Jack, Review – sialons and related nitrogen ceramics, J. Mater. Sci. 11 (1976) 1135–1158.
[6] N. Hirosaki, R.J. Xie, K. Kimoto, T. Sekiguchi, Y. Yamamoto, T. Suehiro, M. Mitomo, Characterization and properties of green-emitting β-SiAlON:Eu^{2+} powder phosphors for white light-emitting diodes, Appl. Phys. Lett. 86 (2005) 211905–211913.
[7] L.H. Liu, R.J. Xie, N. Hirosaki, T. Takeda, C.N. Zhang, J.G. Li, X.D. Sun, Optical properties of blue-emitting $Ce_xSi_{6-z}Al_{z-x}O_{z+1.5x}N_{8-z-x}$ for white light-emitting diodes, J. Electrochem. Soc. 157 (2010) H50–H54.
[8] K. Kimoto, R.J. Xie, Y. Matsui, K. Ishizuka, N. Hirosaki, Direct observation of single dopant atom in light-emitting phosphor of β-SiAlON:Eu^{2+}, Appl. Phys. Lett. 94 (2009) 041908–41913.
[9] Y.Q. Li, N. Hirosaki, R.J. Xie, T. Takeda, M. Mitomo, Crystal and electronic structures, luminescence properties of Eu^{2+}-doped $Si_{6-z}Al_zO_zN_{8-z}$ and $M_ySi_{6-z}Al_{z-y}O_{z+y}N_{8-z-y}$ (M = 2Li, Mg, Ca, Sr, Ba), J. Sol. Stat. Chem. 181 (2008) 3200–3210.
[10] W.W. Chen, Y.B. Cheng, W.H. Tuan, Preparation of sialon-transition metal silicide composites, J. Eur. Ceram. Soc. 26 (2006) 193–199.
[11] H.D. Kim, Y.J. Park, J.W. Koh, B.S. Karunaratne, SiAlON having magnetic properties and method for manufacturing the same, U.S. Patent Appl. Pub. No.: US2009/0314982 A1, 2009.
[12] J.E. Gilbert, A. Mosset, Preparation of β-SiAlON from coal-mine schists, Mater. Res. Bull. 32 (1997) 1441–1448.
[13] J.E. Gilbert, A. Mosset, Preparation of β-SiAlON from fly ashes, Mater. Res. Bull. 33 (1998) 117–123.
[14] J.I. Goldstein, D.E. Newbury, D.C. Joy, C. Lyman, P. Echlin, E. Lifshin, L. Sawyer, J. Michael, Scanning Electron Microscopy and X-ray Microanalysis, third ed., Kluwer-Plenum, New York, 2002.
[15] A.S. Sanyal, J. Mukerji, Mossbauer study of the effect of iron on the synthesis of sialon from clay, J. Mater. Sci. Lett. 5 (1986) 787–788.
[16] H. Mandal, F. Kara, S. Turan, A. Kara, Multication doped alpha-beta SiAlON ceramics, U.S. Patent Appl. Pub. No.: US2004/0067838 A1, 2004.
[17] R. Kumar, N.C. Acıkbas, F. Kara, H. Mandal, B. Basu, Microstructure–mechanical properties-wear resistance relationship of SiAlON ceramics, Metall. Mater. Trans. A 40 (2009) 2319–2332.
[18] C.P. Gazzara, D.R. Messier, Determination of phase content of silicon nitride by X-ray diffraction analysis, Am. Ceram. Soc. Bull. 56 (1977) 777–780.
[19] D.B. Williams, C.B. Carter, Transmission Electron Microscopy, Spectrometry IV, Plenum Press, New York, 1996.
[20] S. Turan, K.M. Knowles, Formation of boron nitride inclusions in hot isostatically pressed silicon nitride–silicon carbide composites, J. Am. Ceram. Soc. 78 (1995) 680.
[21] R.D. Shannon, Revised effective ionic radii and systematic studies of interatomic distances in halides and chalcogenides, Acta Cryst. A32 (1976) 751–767.
[22] R. Dupree, M.H. Lewis, G. Lengward, D.S. Williams, Co-ordination of Si atoms in silicon–oxynitrides determined by magic-angle-spinning NMR, J. Mater. Sci. Lett. 4 (1985) 393–395.
[23] E.I. Yurieva, A.L. Ivanovskii, Electronic structure of 3D-metal impurities in silicon oxynitride, J. Struct. Chem. 42 (2001) 165–171.
[24] J.M. Zuo, J.C. Mabon, Web-based electron microscopy application software Web-EMAPS, Microsc. Microanal. 10 (Suppl. 2) (2004), http://emaps.mrl.uiuc.edu/.
[25] R.F. Egerton, Electron Energy-Loss Spectroscopy in the Electron Microscope, second ed., Plenum Press, New York, 1996.